Mineralia Slovaca, Web ISSN 1338-3523, ISSN 0369-2086
52, 1 (2020), 33 – 44, © Authors 2020. CC BY 4.0

Differential stresses estimated from calcite veins in HP-LT Triassic Hallstatt Limestones (Northern Calcareous Alps, Austria)

BARBORA ŠČERBÁKOVÁ[1], HANS-JÜRGEN GAWLICK[2] and ZOLTÁN NÉMETH[3]

[1]Technical University Košice, Faculty of Mining, Ecology, Process Control and Geotechnology, Letná 9, SK-042 00 Košice, Slovakia; barbora.zakrsmidova@gmail.com
[2]Montanuniversität Leoben, Department of Applied Geosciences and Geophysics, Petroleum Geology, Peter Tunner Str. 5, A-8700 Leoben, Austria; gawlick@unileoben.ac.at
[3]State Geological Institute of Dionýz Štúr, Mlynská dolina 1, SK-817 04 Bratislava, Slovakia; zoltan.nemeth@geology.sk

Abstract: Using paleopiezometry we calculated differential stresses ($\sigma_D = \sigma_1 - \sigma_3$), recorded by calcite veins during final stages of deformation of exhumed HP-LT Triassic Hallstatt Limestone blocks in the Pailwand Mt. (central Northern Calcareous Alps). Extreme recrystallization of the micrite of Hallstatt Limestone, which had taken place earlier than the studied calcite veins originated, has not allowed us to use calcite paleopiezometry on host rock. Studied calcite veins were strained during the last deformation phase which the Hallstatt Limestone has underwent. High number of deformation twins per 1 mm in calcite grains (Twin Density; D = 21−47) with grain-size from 323 to 571 μm demonstrates the deformation at differential stresses from 184 to 234 MPa.

This paper supports earlier interpretation that the Hallstatt Limestone in the Northern Calcareous Alps represents a lateral equivalent of a part of the Bôrka nappe of Meliata unit in the Western Carpathians and both segments underwent Middle Jurassic subduction, followed by rapid Late Jurassic-Early Cretaceous exhumation and thrusting.

Key words: paleopiezometry, differential stress, calcite, Hallstatt Mélange, Eastern Alps, Meliata Unit, Western Carpathians

Graphical abstract

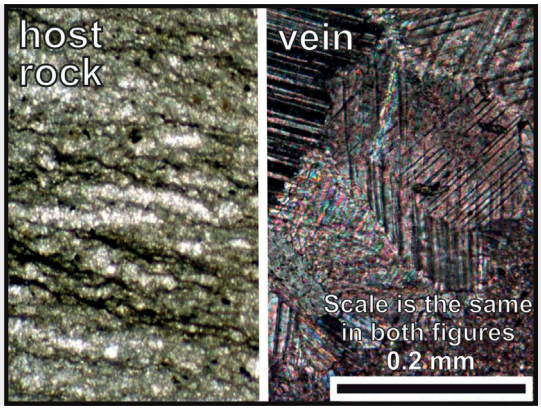

Highlights

- Research results contribute to further testing and upgrading of the methodology of calcite paleo-piezometry, as well as reconstruction of Cenozoic tectono-metamorphic events in E. Alps and W. Carpathians
- New paleopiezometric results (184–233 MPa) from the calcite veins in the Hallstatt Limestone Succession, as a lateral analogue of the Bôrka nappe rock succession of Meliatic unit (W. Carpathians), have completed the earlier paleopiezometric data – differential stresses acting during subduction (348–430 MPa) and exhumation (188–278 MPa) in the Bôrka nappe.

Introduction

Southern zones of the Northern Calcareous Alps and the Western Carpathians represented in Triassic to Middle Jurassic time the northwestern shelf of the Neotethys (in this paper named as Meliata-Hallstatt) Ocean, striking from the Western Carpathians at least to the Hellenides (Fig. 1). According to one-ocean paleogeographic and geodynamic reconstructions (e.g. Krystyn & Lein in Haas et al., 1995; Gawlick et al., 1999, 2008; Schmid et al., 2008; Missoni & Gawlick, 2011a, b), the formation of Jurassic mélanges and an accretionary wedge is a result of a northwestward propagating thin-skinned orogen with the Middle to early Late Jurassic ophiolite obduction (i.e. Frisch & Gawlick, 2003; Plašienka, 2018, with references therein). Parts of the former outer shelf (Fig. 1: Meliata, Hallstatt and Zlambach facies zones) became imbricated, subducted and underwent a high-pressure–low-temperature metamorphism (Faryad, 1999; Faryad & Henjes-Kunst, 1997; Gawlick & Höpfer, 1999; Mock et al., 1998; Németh et al., 2012). From the Tithonian onwards, these metamorphosed slices were being exhumed.

Studied metamorphosed Triassic Hallstatt Limestones of the Pailwand Mt. (Figs. 2 and 3) are located roughly 50 km SE of Salzburg on the NE edge of the Tennengebirge Mts. They rest on the uppermost part of the Hallstatt

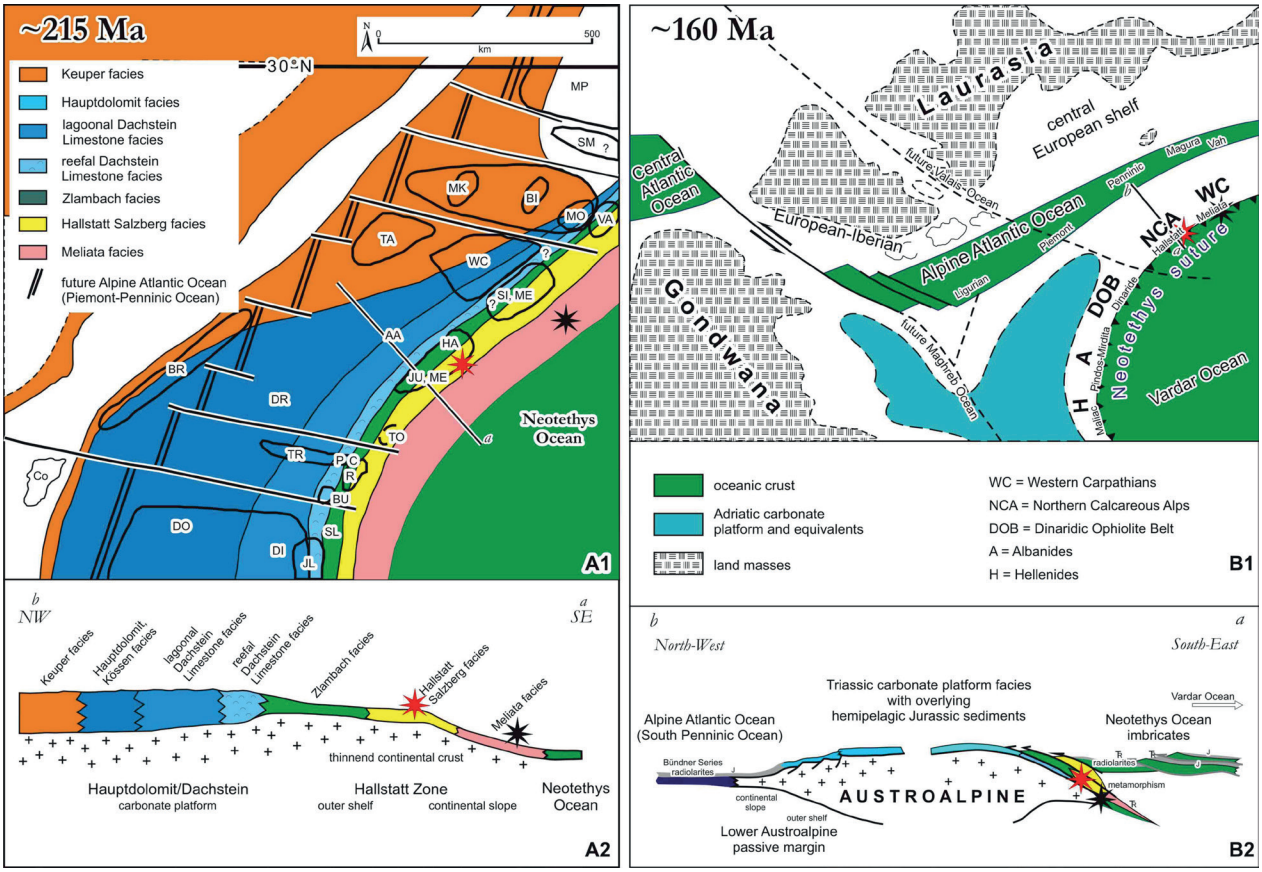

Fig. 1. ***A1*** – Paleogeographic reconstruction and facies distribution of the northwestern Neotethys realm in the Late Triassic time (paleogeographic position of the Austroalpine realm modified after Krystyn & Lein in Haas et al., 1995). *AA* Austroalpine; *BI* Biharia; *BR* Briançonnais; *BU* Bükk; *C* Csovar; *Co* Corsica; *DI* Dinarides; *DO* Dolomites; *DR* Drau Range; *HA* Hallstatt; *JU* Juvavicum; *JL* Julian Alps; *ME* Meliaticum; *MK* Mecsek; *MO* Moma Unit; *MP* Moesian platform; *P* Pilis-Buda; *R* Rudabanyaicum; *SI* Silicicum; *SL* Slovenian trough; *SM* Serbo-Macedonian Unit; *TA* Tatricum; *TO* Tornaicum; *TR* Transdanubian Range; *VA* Vascau Unit; *WC* - more internal zones of Western Carpathians located closer to Neotethys basin. ***A2*** – Schematic cross section through the Neotethys passive continental margin of the Austroalpine realm in the Late Triassic showing a typical passive continental margin facies distribution. ***B1*** – Paleogeographic position of the Northern Calcareous Alps as a part of the Austroalpine domain around the Middle/Late Jurassic boundary (after FRISCH, 1979). In this reconstruction, the Northern Calcareous Alps represent part of the Jurassic Neotethyan Belt (orogen) striking from the Carpathians to the Hellenides (Missoni & Gawlick, 2011a). The Neotethys suture is an equivalent to the West-Vardar ophiolite obduction (e.g., Dinaridic Ophiolite Belt) in the sense of Schmid et al. (2008) = far-travelled ophiolite nappes of the western Neotethys Ocean in the sense of Gawlick et al. (2008). The eastern part of the Neotethys Ocean remained open = Vardar Ocean (compare Missoni & Gawlick, 2011a). Toarcian to Early Cretaceous Adria-Apulia carbonate platform and equivalents are visualized according to Golonka (2002), Vlahovič et al. (2005) and Bernoulli & Jenkyns (2009). ***B2*** – Schematic cross section of the Austroalpine realm along the Alpine Atlantic margin towards the Neotethys realm around the Middle/Late Jurassic boundary showing the formation of the Neotethyan Belt (Missoni & Gawlick, 2011a). Red stars = study area, Pailwand. Black stars = comparison with the Bôrka nappe of the Meliatic Unit.

Mélange of the Lammer Basin, striking from the Saalach Unit in the west to the Gosaukamm Mt. in the east (e.g. Missoni & Gawlick, 2011a). Metamorphosed Hallstatt Limestone tectonic blocks occur on the top of the Middle to early Late Jurassic basin fill due to their northwest trending displacement. The Pailwand Mt. consists of amalgamated tectonic blocks of differing paleogeographic provenance and different diagenetic overprint ((see details in Gawlick & Königshof, 1993, and Gawlick & Höpfer, 1999).

The Hallstatt Limestone Succession metamorphic overprint in the Pailwand area, revealed by the Conodont Colour Alteration Index (CAI), calcite-dolomite solvus thermometry and the chlorite composition (clinochlore or pycnochlorite) with Al^{IV} = 1.10–1.20 pfu (Gawlick & Königshof, 1993; Kralik et al., 1987; Gawlick & Höpfer, 1999; Frank & Schlager, 2006) took place at peak temperature 360–480 °C for the host rock recrystallization (CAI > 5.5 and CAI 6.0), The minimum pressures of 6–8 kb at 360 °C or 10 kb at 400 °C were deduced by microprobe analyses of the texturally different white micas with high celadonite content of 3.35–3.45 Si pfu. The metamorphic overprint of 155–152 Ma (Kimmeridgian) was determined by K-Ar and Rb-Sr on mica from fault

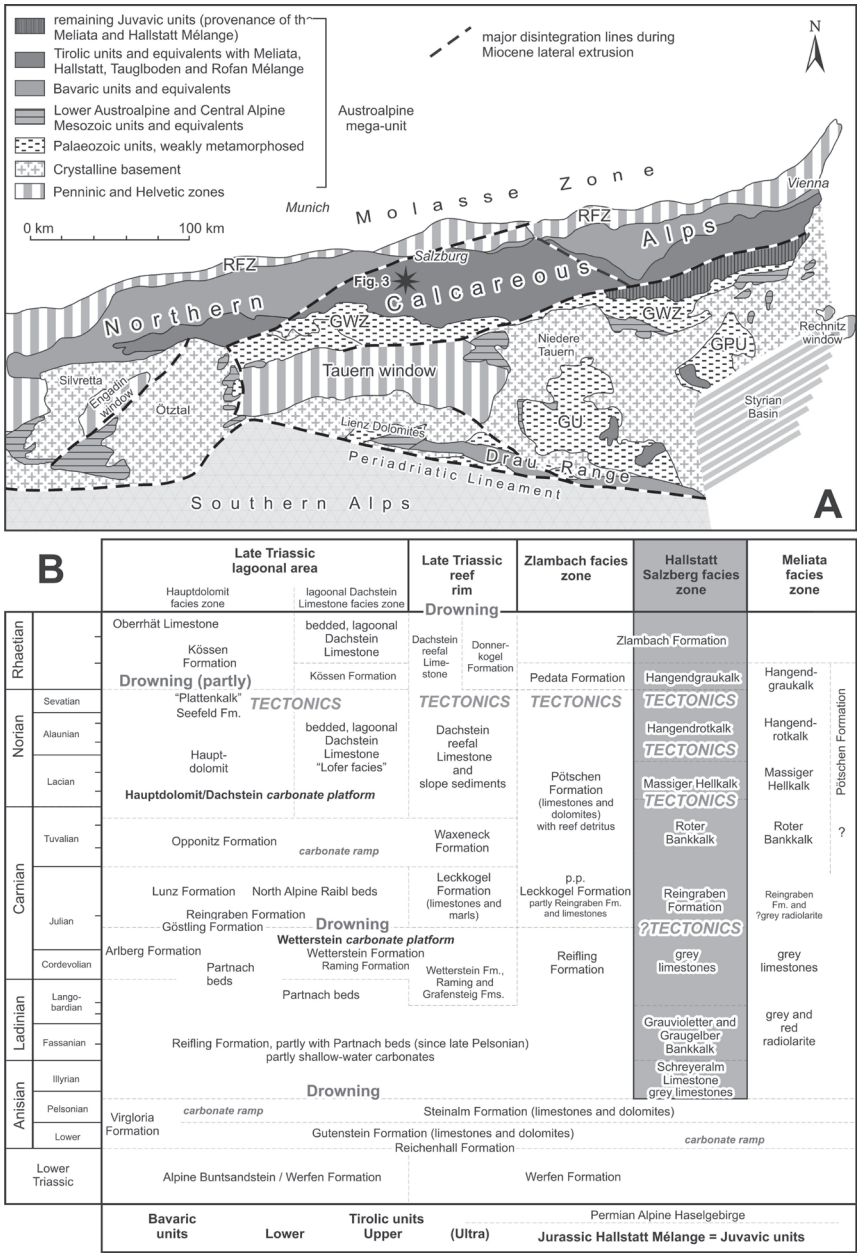

Fig. 2. ***A*** – Tectonic sketch map of the Eastern Alps with the Northern Calcareous Alps in their northern part showing the location of the study area (after Tollmann, 1977, and Frisch & Gawlick, 2003). *GPU* – Graz Paleozoic Unit. *GU* – Gurktal Unit. *GWZ* – Greywacke Zone. *RFZ* – Rhenodanubian Flysch Zone. Star indicates location of Fig. 3. ***B*** **–** Stratigraphic table of the Triassic formations and tectonic events in the Northern Calcareous Alps and equivalents (modified after Missoni & Gawlick, 2011a, b); compare Tollmann (1976). The Hallstatt Limestone Succession of the Pailwand is marked in grey.

gouges in the Hallstatt Limestones (Kralik et al., 1987), or a wide spectrum of Ar-Ar dating on mica (Frank & Schlager, 2006), providing the age clusters between 163–152 Ma and 141–132 Ma, as well as younger ages.

Recent research was motivated by previous studies in the HP-LT sequences of the Bôrka nappe in the Western Carpathians (Németh, 1996, 2005; Németh et al., 2007, 2012), aiming to obtain paleopiezometric data also from HP-LT Hallstatt Limestones of the Eastern Alps as a part of the Neotethyan Belt, too. This paper presents differential stress values ($\sigma_D = \sigma_1 - \sigma_3$) from calcite veins as products of the last stages of deformation of HP-LT Triassic Hallstatt Limestones of Pailwand Mt., because the very fine-grained (mylonitized) calcite grains (< 10 μm) in sheared layers in open-marine fine-grained Hallstatt Limestones of Pailwand (Fig. 4) did not allow application of paleopiezometry. Therefore, our research was focused on the youngest generation of calcite veins, penetrating the limestones, as well as penetrating older calcite veins, formed during an earlier stage of the diagenetic history of the Hallstatt Limestone Succession prior to their burial (Gawlick & Höpfer, 1999). The relative age of calcite veins was distinguished by overprinting relations.

Methodology of paleopiezometry

The method of paleopiezometry, applied on deformed calcite grains – either in the calcitic marbles or calcite veins, allows to estimate paleo-stress, being expressed by the differential stress ($\sigma_D = \sigma_1 - \sigma_3$; *MPa*). The method is best calibrated for mono-mineral calcite marbles with a pervasive ductile deformation (Rowe & Rutter, 1990) and is useful for establishing the deformation gradient e.g. in a profile across a shear zone, or a normal or reverse fault plane with ductile deformation, The paleopiezometric measurements are based on the approaches by Jamison & Spang (1976), Lacombe (2007) and Laurent et al. (2000), who assume that the critical resolved shear stress (CRSS; τ_c) is constant – about 10 MPa. According to Burkhard (1993), the deformation twins are developed at very low shear stress varying in between τ_c = 2–12 MPa, what is depending on temperature, as well as the pressure conditions. The stress required to activate twinning is likely varying with the shear modulus and decreases with temperature (Rowe & Rutter, 1990). In general, the twinning represents one of

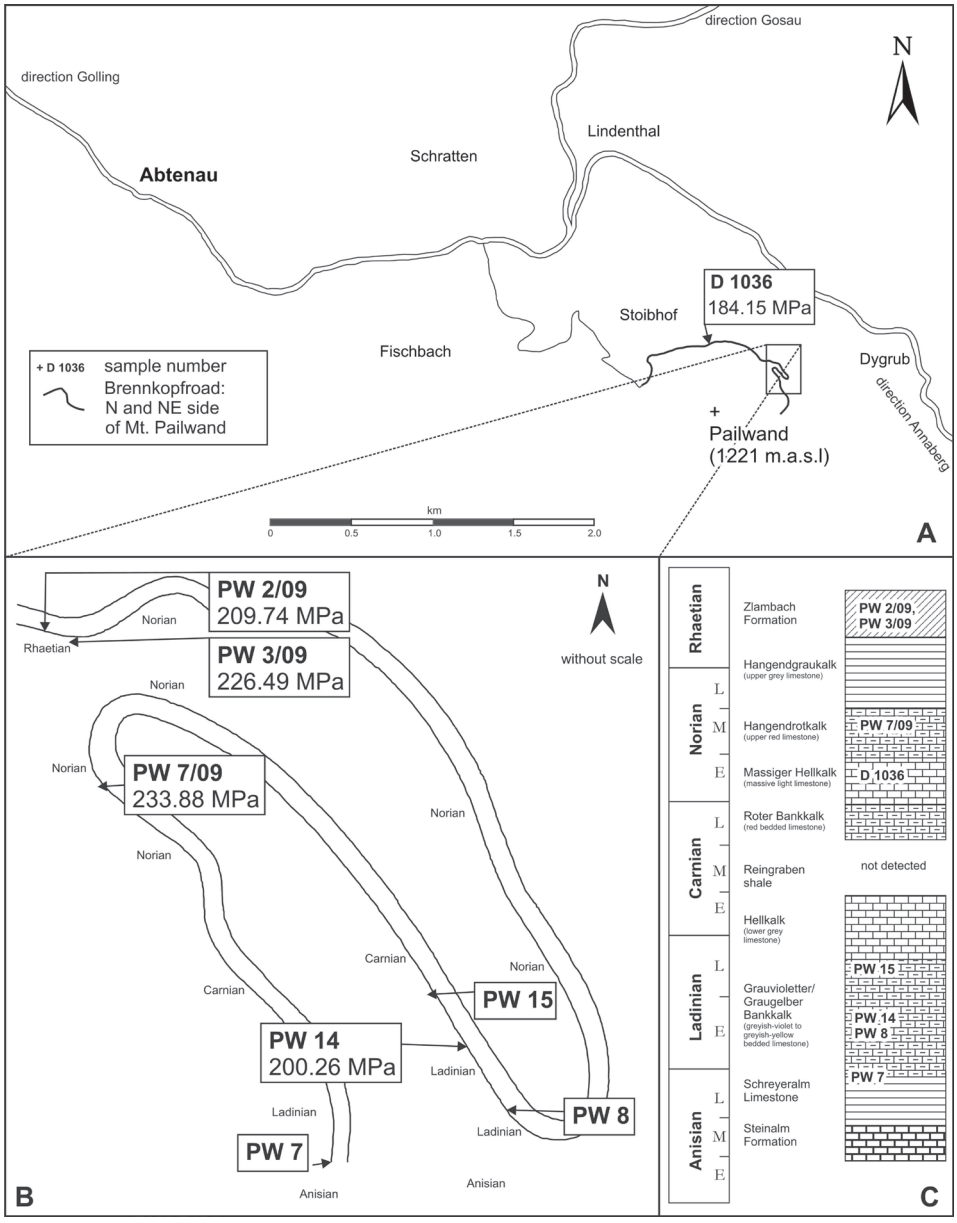

Fig. 3. ***A*** – Location of the study area in the southwestern central Northern Calcareous Alps east of Abtenau and the sample localities. ***B*** – Hallstatt Limestone Succession along the forest road at the northeastern side of Mt. Pailwand. Studied samples have added the values of differential stresses revealed in this study. ***C*** – Anisian to Rhaetian Hallstatt Limestone Succession of the Pailwand block and stratigraphic position of the studied samples.

important deformation mechanisms at LT-HP conditions (Groshong, 1972, 1988; Christian & Mahajan, 1995; Burckhard, 1993; Ferrill et al., 2004; Turner, 1964). The start of twinning is connected with the stress concentration on calcite crystals surfaces, grain boundaries, or various defects. Growth of twins is parallel to the twin boundary (Burkhard, 1993; Christian & Mahajan, 1995; Nicolas & Poirier, 1976).

Calcite paleopiezometry takes into account the size of recrystallized grains and the number and type of deformation twins. According to Rowe & Rutter (1990), there are two main independent ways for determining the differential stresses in calcitic rocks – the methods of *twinning incidence (I_t = twinned grains / No. of grains total)* and *twin density (D = No. of twins / diameter of grains)*, both in *MPa*. (l.c.).

Twinning incidence, I_t, is defined as a percentage of grains having microscopically visible twins. Differential stress σ_D ($\sigma_1 - \sigma_3$; MPa) can be estimated by the equation below, where d represents the size of grains in μm. The standard error in this technique, determined by Rowe & Rutter (1990), is up to 31 MPa.

$$\sigma_D = 523 + 2.13\ I_t - 204 \log d\ [MPa]$$

Twin density, D, is defined as the number of twins regarding the grain diameter, measured perpendicularly to the twins. As demonstrated by Friedman & Heard (1974), as well as Rybacki et al. (2013), twin density measurements

using a flat stage match those measured with the U-stage to within 10 %. The standard error of this method is 43 MPa (Rowe & Rutter, 1990). The relation of the differential stress on twin density D is as follows:

$$\sigma_D = -52.0 + 171.1 \log D \text{ [MPa]}$$

To guarantee maximum representativeness of data, measurements were done systematically on profiles through thin sections, taking into account each neighbouring grain. Extreme dimensions (extremely small or large grains) were excluded from following calculations, using the variation coefficient 0.25 (Ranalli, 1984). Numerical processing used a procedure consisting of several steps (cf. Németh, 2005):

1. Separation and batching of obtained data according to the grain size.
2. Counting the number of grains in individual size categories, the grains without twins, as well as with twins. Values are used for calculation of twinning incidence I_t.
3. Counting of the number of twins in individual size categories and sums of all perpendicular diameters of grains related to twins. Values are used for calculation of twin density D.

For the maximum correctness, the calculation has been realized by six ways. Four calculations applied the variation coefficient below 0.25 (± 25 %; Ranalli, 1984), avoiding inaccuracy of results by calculations with extremely small and large grains.

Multiple determination of the differential stress by the method of Twinning Incidence:

1. Differential stresses have been calculated separately for each grain size class. The total differential stress has been calculated as their weighted mean. The variation coefficient was not implemented into calculations in this particular case.
2. Calculation with the total twinning incidence (without selective calculation for each grain size). Calculation with the coefficient of variation.
3. Determination of differential stress by the arithmetic mean from the partial results for individual categories. Calculation with the coefficient of variation.
4. Determination of differential stress by the weighted mean from the partial results for individual categories. Calculation with the coefficient of variation.

Multiple determination of the differential stress using method of Twin Density:

5. Calculation with application of mathematically determined twins number with respect to grain sizes perpendicular to twins without separation of calculation for individual size classes. The coefficient of variation was not implemented into calculation in this particular case.
6. The same way of calculation with implemented coefficient of variation.

In most of samples, results of both methods (Twinning Incidence and Twin Density), were comparable. Because a greater number of measured parameters, the Twin Density Method we consider as more precise and obtained results (with implementation of the coefficient of variation by Ranalli, 1984) seems to be well applicable for tectonic considerations.

Results

The open-marine fine-grained metamorphosed Hallstatt Limestones have preserved a strong tectono-metamorphic and ductile deformation overprint, represented in some layers by very fine-grained (mylonitized) calcite crystals with grain-size of < 10 μm (Fig. 4). Such mylonites were not appropriate for paleopiezometric research. Therefore our attention was focused on younger calcite veins, bearing deformation twins (Fig. 5), which originated and were deformed later than the ductile deformation of the host rock occurred.

Generally 1–5 mm thick calcite veins (PW-2/09, PW-3/09, PW-7/09, PW-14 and D-1036; Figs. 3 and 5) were hosted by Hallstatt Limestone samples, which have an exact age control (Fig. 3C), and were used by one of authors (HJG) in his previous research.

Our systematic counting of the grain-size (d) and a number of deformation twins in 240 calcite grains along lines perpendicular to studied veins in thin sections has provided following results: the representative grain-sizes of calcite grains in veins are 323–571 μm, the twinning incidents determined by variation coefficient are 29–100, the numbers of twins per 1 mm of perpendicular diameter are 21–47 and calculated differential stresses are 184 to 234 MPa (Tab. 1).

Because twinning can accommodate only a limited amount of strain and always operates in specific crystallographic directions, if occurs the larger strain it can be accommodated by additional pressure solution dislocation creep or recrystallization (cf. Passchier & Trouw, 1996). In studied thin sections we have found also manifestations of three dislocation creep regimes of dynamic recrystallization (Fig. 5; cf. e.g. Dunlap et al. (1997), Stöckhert et al. (1999) and Zulauf (2001)) – the grain boundary area migration (GBAR), bulging (BLG) and sub-grain rotation (SGR), so the total differential stress can be even higher than that revealed by paleopiezometry.

Sample D-1036 with the mean grain-size diameter 515 μm, providing the lowest value of the differential stress (σ_D = 184 MPa), contains also polygonal grains. They characterize the process of recovery with static recrystallization induced by temperature increase. The

Tab. 1

The results of Twinning Incidence (It) and Twin Density (D) paleopiezometric methods.

		TWINNIG INCIDENCE (It)					TWIN DENSITY (D)		
	Representative grain-size	Calcul. without variation coeffic.	It for interval determined by variation coefficient	Calculation with variation coefficient			D – no. of twins per 1 mm of perpend. diameter	Calcul. without variation coeffic.	Calculat. with variation coeffic.
		Calculat. with weight. mean		Calculat. with the whole It	Arith. mean of σ for size classes	weight. mean of σ for size classes			
	µm	σ_D (MPa)		σ_D (MPa)	σ_D (MPa)	σ_D (MPa)		σ_D (MPa)	σ_D (MPa)
PW-2/09	465.87	195.72	100	191.67	194.37	195.72	34	218.57	**209.74**
PW-3/09	365.26	360.24	20.68	44.29	38.49	38.49	21	215.31	**226.49**
PW-7/09	323.38	119.76	29.41	73.67	92.99	92.99	47	222.95	**233.88**
PW-14	571.25	200.26	76.92	124.45	121.97	124.81	30	189.51	**200.26**
D 1036	515.38	144.38	78	135.87	151.82	150.39	24	191.25	**184.15**

Note: Table presents the results of several ways of calculation of differential stresses (σ_D) in the studied samples from Pailwand (explained in the text). The results of Twin Density method, processed with the variation coefficient (the last right column), we suppose the most objective and applicable for further considerations.

Fig. 4. Deformation characteristics and microfacies of the Hallstatt Limestones of the Pailwand.

a – Early Ladinian Hallstatt Limestone. Sample **PW 8**. Sheared and recrystallized originally micritic limestone with filaments and radiolarians (see **b**). In the central part the original microfacies occur. In zones with the ductile deformation the limestone is totally recrystallized (see **c**). Scale bar = 500 µm.

b – Enlargement of **a** showing the well preserved microfacies characteristics of the filament-radiolarian wackestone. The preservation of the filaments and radiolarians is strongly affected by recrystallization. Scale bar = 150 µm.

c – Enlargement of **a** – sheared and totally recrystallized limestone. The extremely fine grain-size of this ultramylonitic limestone with signs of pressure solution and the absence of deformation twins do not allow to apply paleopiezometry. Scale bar = 75 µm.

d – Late Anisian Hallstatt Limestone. Sample **PW 7**. Shear zone in the original nodular limestone with ductile shearing and ultra-stylolitization. Whereas in the light grey parts the microfacies is well preserved, the calcite grains in the shear zone are completely mylonitized (see **e**). Scale bar = 500 µm.

e – Enlargement of **d** showing the completely recrystallized and mylonitized calcite crystals. Scale bar = 150 µm.

f – Late Anisian Hallstatt Limestone. Sample **PW 7**. Contact of a ductile deformed and recrystallized shear zone with a surrounding limestone matrix. In the lower part of the picture the limestone is practically not affected by shearing, having quite well preserved original microfacies. The rim of the shear zone is characterized by strong recrystallization and ultra-stylolitization. The central part of presented thin section represents the core of the shear zone with completely ductile recrystallized calcite grains. The asymmetric structures and porphyroclasts rotation are visible. Scale bar = 150 µm.

g – Sample **PW 7**. Completely recrystallized calcite grain in the shear zone showing newly formed phengites (greenish) at the rim of numerous sub-grains. In some cases (right and bottom parts of the calcite grain) the phengite forms larger accumulations. Scale bar = 150 µm.

h – Late Ladinian Hallstatt Limestone. Sample **PW 15**. Ductile deformed filament limestone showing complete recrystallization in the deformed parts. In the larger clasts the radiolarian and filaments ghosts are visible. Frequent porphyroclasts of sigma- and delta-type. Scale bar = 150 µm.

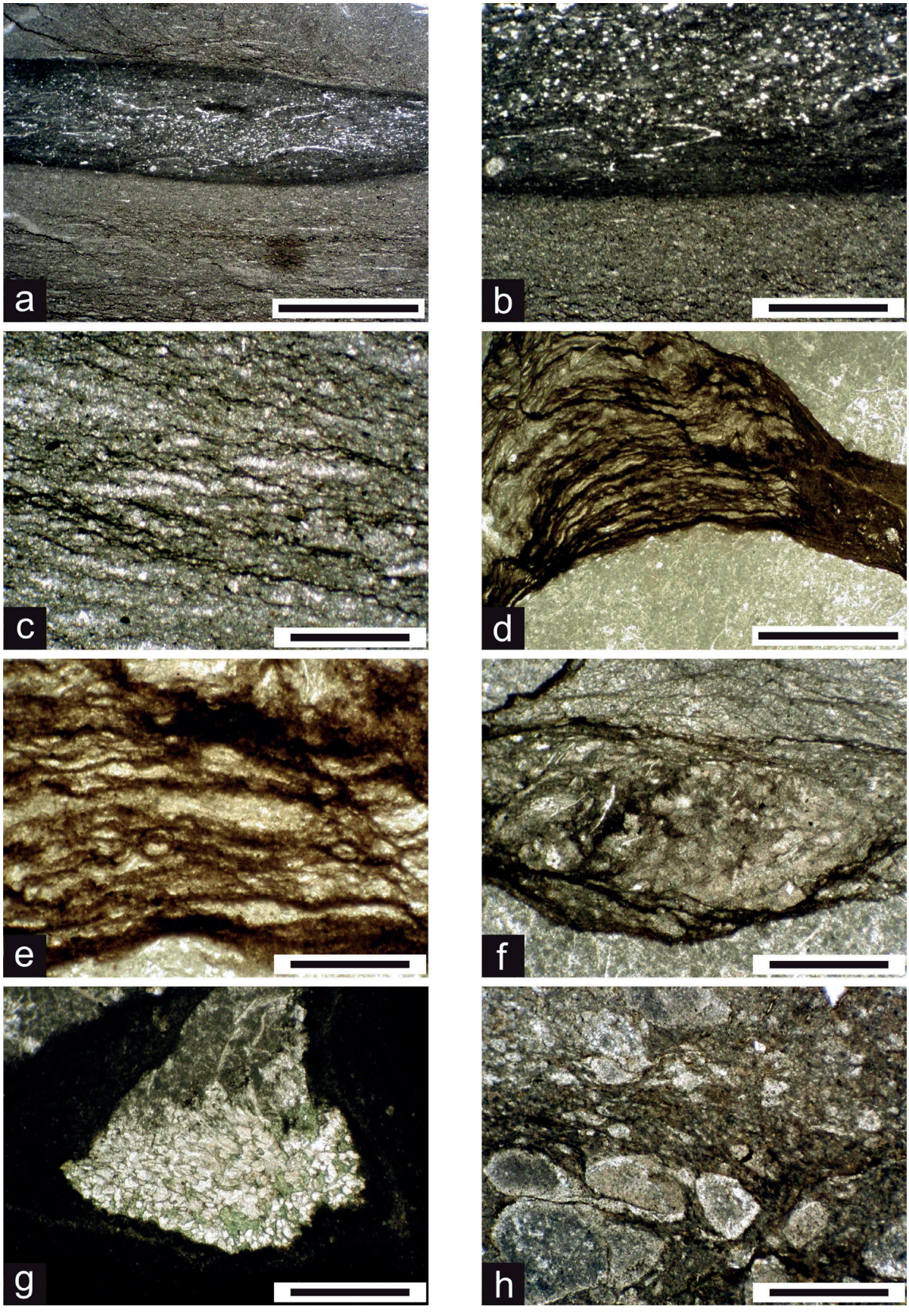
a
b
c
d
e
f
g
h

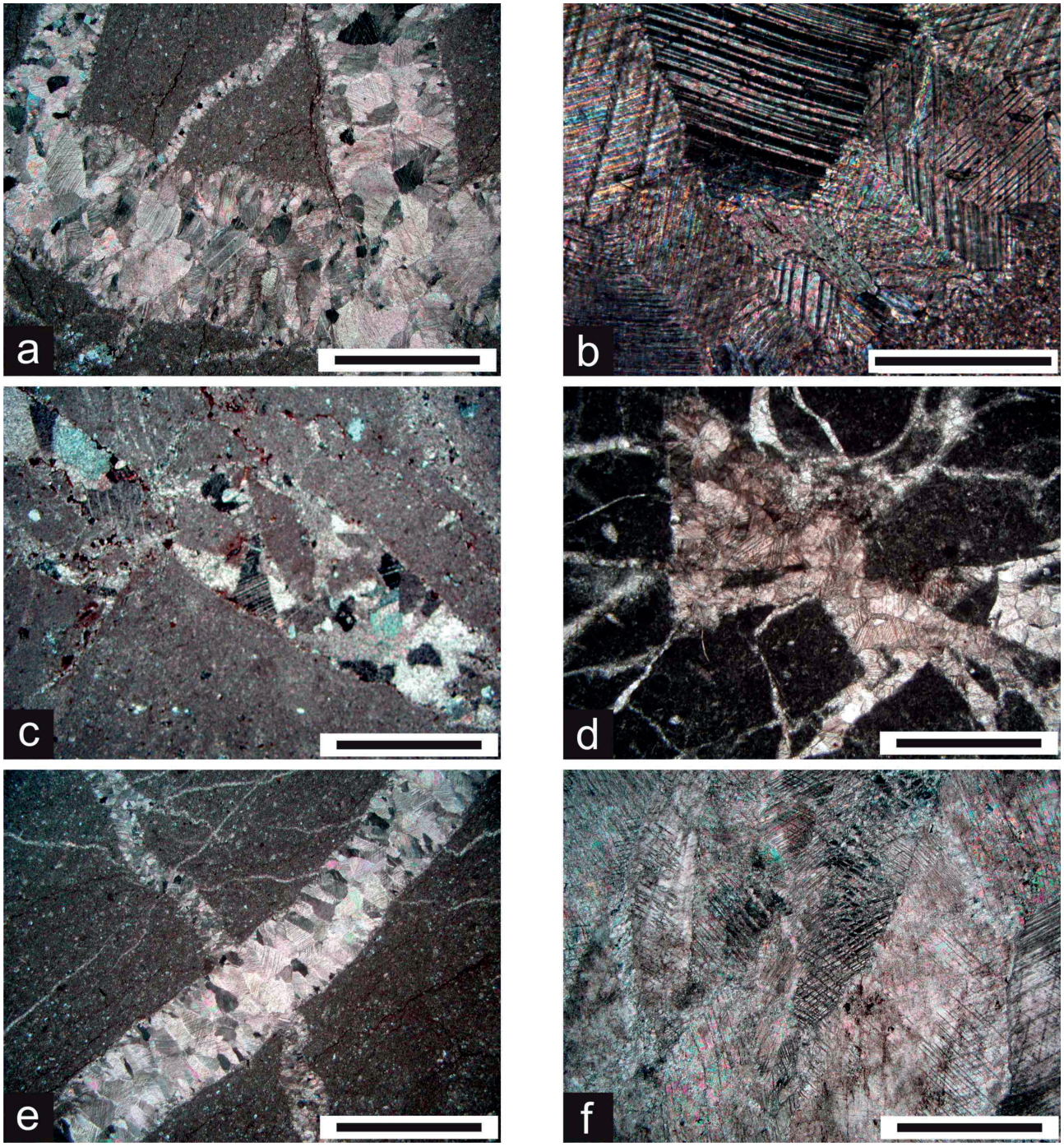

Fig. 5. Microphotographs of studied calcite veins. Description bellow relates the following parameters: d – average grain-size, It – Twinning incidence – the percentage of grains with deformation twins; D – Twin density – the average number of twins per 1 mm perpendicular to twin lamellae; σ_D – differential stress (MPa). Compare Tab. 1.

a, b – Sample **PW 2/09**: d = 466 μm; It = 100 %; D = 219 MPa; σ_D = 210 MPa. Scale bars = 2 mm (in a) and 200 μm (in detail b).

c – Sample **PW 3/09**: d = 365 μm; It = 21 %; D = 215 MPa; σ_D = 227 MPa. Scale bar = 2 mm.

d – Sample **PW 7/09**: d = 323 μm; It = 29 %; D = 232 MPa ; σ_D = 234 MPa. Scale bar = 2 mm.

e – Sample **PW 14**: d = 571 μm; It = 77 %; D = 190 MPa; σ_D = 200 MPa. Scale bar = 2 mm.

f – Sample **D 1036**: d = 515 μm; It = 78 %; D = 191 MPa; σ_D = 184 MPa. Scale bar = 200 μm.

increasing grain-size diameter (d) causes the decrease of differential stresses (σ_D), what is depicted in Tab. 1.

Discussion

The Hallstatt Mélange in the southern zone of Northern Calcareous Alps (Frisch & Gawlick, 2003), as well as the Meliata Mélange, incl. the Bôrka nappe, resting on Gemeric Unit in the Western Carpathians (cf. Mello et al., 1998), represent two lateral parts of the Neotethyan orogenic belt (Missoni & Gawlick, 2011a).

For the metamorphosed rocks of the Meliata unit, included into the Bôrka nappe, numerous thermobarometric and geochronological data are available (Faryad, 1995; Faryad & Henjes-Kunst, 1997; Faryad & Hoinkes, 1999; Aubrecht et al., 2010; Ivan, 2002; Ivan et al., 2009; Ivan & Méres, 2009; Dallmeyer et al., 1993, 1996, 2005, 2008; Maluski et al., 1993; Putiš et al., 2011, 2012, 2014, 2019; Plašienka et al., 2019), depicting a Jurassic higher pressure overprint in the subduction process (170–150 Ma). In contrast, in the Northern Calcareous Alps the thermobarometric and geochronological data are scarce due to the fact, that carbonates represent practically the only preserved metamorphosed rocks, and more variegated rock suite and mineral asseblages for thermobarometry are absent (Gawlick & Frisch, 2003, with references therein).

Earlier paleopiezometric research of recrystallized limestones from the Bôrka nappe in the Western Carpathians (cf. Németh, 2005; Németh et al., 2012), has provided the peak differential stresses (348–430 MPa; l.c.), related to ductile deformation in the subduction slab. As interpreted by l.c., the recrystallization state of the rock, manifesting high differential stresses, was "frozen" by fast exhumation and they are recently positioned in the frontal part of the Bôrka nappe. The stresses in the subduction slab during later stages of exhumation were lowered probably due to the convection mantle heat input (cf. Németh et al., 2016; Zákršmidová et al., 2016), so ongoing static recrystallization lowered the differential stress (188–278 MPa; Németh, 2005).

Evolution in Pailwand we expect similar like in the Bôrka nappe, so it motivated us to document it by paleopiezometric data from both segments, resp. combine data if some are missing in one of these two segments.

We assume that in the case of studied Hallstatt Limestones, the differential stresses 184–234 MPa (Tab. 1) of deformed grains in penetrative calcite veins document the last stage of exhumation, similarly like it was found in the Bôrka nappe of Meliatic unit, whereas the earlier higher pressure metamorphism of continual subduction-exhumation process in the Hallstatt Limestones is manifested by their mylonitization / ultramylonitization (cf. Fig. 4; extreme grain-size reduction, origin of asymmetric shape of porphyroclasts, etc., origin of micro-shear zones). The grains (porphyroclasts), which originated in this higher pressure process, are so small which hinder to application of paleopiezometric measurements according to method by Rowe & Rutter (1990). It was the reason of focussing our paleopiezometric research on calcite grains in penetrative thin veins (thickness of 1–5 mm), which origin can be tied with the final stage of subduction-exhumation process when the dynamic recrystallization of calcite in veins was followed with the beginning of static recrystallization. This process was dated to (1) 146–135 Ma or (2) ~119–113 Ma (cf. Frank & Schlager, 2006). The first age group indicates an exhumation of the Neotethyan Belt (Missoni & Gawlick, 2011a) and the second group is related to the so-called Eo-Alpine evolution (cf. Frank & Schlager, 2006).

Conclusions

The paleopiezometric investigation on deformed calcite veins within a metamorphosed Hallstatt Limestone Succession in the central Northern Calcareous Alps has

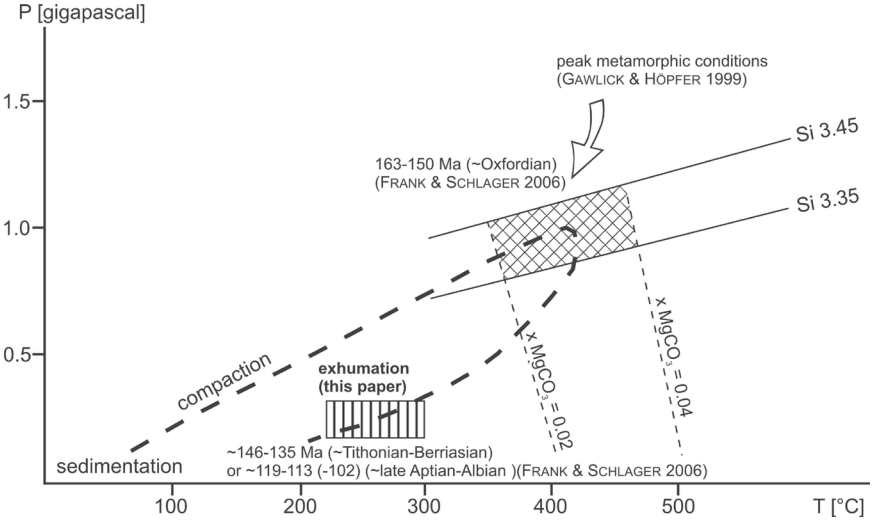

Fig. 6. Pressure-temperature path of subduction and exhumation of the Hallstatt Limestone Succession in the Pailwand area. Data from: Gawlick & Höpfer (1999), Frank & Schlager (2006) and this study

provided numeric data about the differential stresses ($\sigma_D = \sigma_1 - \sigma_3$) from the final stages of ductile deformation of the calcite veins, close to the onset of their static recrystallization. The number of deformation twins per 1 mm of perpendicular diameter of the grain (Twin Density, D = 21–47) at the grain-size (323–571 μm) has been produced by the deformation at differential stresses σ = 184–234 MPa. Recent paleopiezometric results from the calcite veins in the Hallstatt Limestone Succession, being interpreted as a lateral analogue of the corresponding rock succession in the Bôrka nappe of Meliatic unit in the Western Carpathians, have completed earlier paleopiezometric data – differential stresses acting during subduction process (348–430 MPa) and exhumation (188–278 MPa), revealed by previous research (Németh, 2005; Németh et al., 2012).

Acknowledgements

Grants in the frame of the CEEPUS CIII-RO-0038 network for Barbora Zákršmidová (Ščerbáková) are gratefully acknowledged.

References

Aubrecht, R., Gawlick, H. J., Missoni, S., Suzuki, H., Plašienka, D., Kronome, K. & Kronome, B., 2010: Middle Jurassic matrix radiolarians from the Meliata ophiolite mélange at the type Meliatic sites Meliata and Jaklovce (Western Carpathians): Paleogeographic evidence. *Geol. Balcanica, 39, 33–34.*

Bernoulli, D. & Jenkyns, H., 2009: Ancient oceans and continental margins of the Alpine-Mediterranean Tethys: Deciphering clues from Mesozoic pelagic sediments and ophiolites. *Sedimentology, 56, 149–190.*

Burkhard, M., 1993: Calcite twins, their geometry, appearance and significance as stress-strain markers and indicators of tectonic regime: a review. *J. struct. Geol., 15, 351–368.*

Christian, J. V. & Mahajan, S., 1995: Deformation twinning. *Progress Mater. Sci., 39, 1–157.*

Dallmeyer, R. D., Neubauer, F. & Pitiš, M., 1993: $^{40}Ar/^{39}Ar$ mineral age controls for the pre-Alpine and Alpine tectonic evolution of nappe complexes in the Western Carpathians. In: Pitoňak, P. & Spišiak, J. (eds.): Pre-Alpine Events in the Western Carpathians' Realm. *Stará Lesná, Confer. Excursions Guide, 11–20.*

Dallmayer, R. D., Neubauer, F., Handler, R., Fritz, H., Muller, W., Pana, D. & Putiš, M., 1996): Tectonothermal evolution of the internal Alps and Carpathians: Evidence from $^{40}Ar/^{39}Ar$ mineral and whole-rock data. *Eclogae geol. Helv., 89, 203–227.*

Dallmeyer, R. D., Németh, Z. & Putiš, M., 2005: Regional tectonometamorphic events in Gemericum and adjacent units (Western Carpathians, Slovakia): Contribution by the $^{40}Ar/^{39}Ar$ dating. *Slovak Geol. Mag., 11, 2–3, 155–163.*

Dallmeyer, R. D., Neubauer, F. & Fritz, H., 2008: The Meliata suture in the Carpathians: Regional significance and implications for the evolution of high-pressure wedges within collisional orogens. *J. Geol. Soc., London, 298, 101–115.*

Dunlao, W. J., Hirth, G. & Teyssier, C., 1997: Thermodynamical evolution of a ductile complex. *Tectonics, 16, 983–1000.*

Faryad, S. W., 1995: Phase petrology and P-T conditions of mafic blueshists from the Meliata Unit, West Carpathians, Slovakia. *J. Metamorph. Geol., 13, 701–714.*

Faryad, S. W., 1999: Exhumation of the Meliata high-pressure rocks (Western Carpathians): Petrological and structural records in blueshists. *Acta Montan. Slovaca, 2, 137–144.*

Faryad, S. W. & Henjes-Kunst, F., 1997: Petrological and K-Ar and Ar-40-Ar-39 age constraints for the tectonothermal evolution of the high-pressure Meliata unit, Western Carpathians (Slovakia). *Tectonophysics, 280, 141–156.*

Faryad, S. W. & Hoinkes, G., 1999: Two contrasting mineral assemblages in the Meliata blueshists, Western Carpathians. *Min. Mag., 63, 489–501.*

Ferrill, D. A., Morris, A. P., Evans, M. A., Burkhard, M., Groshong, R. H. J. & Onasch, C. A., 2004: Calcite twin morphology: A low-temperature deformation geothermometer. *J. struct. Geol., 26, 8, 1521–1529.*

Frank, W. & Schlager, W., 2006: Jurassic strike slip versus subduction in the Eastern Alps. *Int. J. Earth. Sci., 95, 431–450.*

Friedman, M. & Heard, H. C., 1974: Principal stress ratios in Cretaceous limestones from Texas Gulf Coast. *Bull. Amer. Assoc. Petrol. Geol., 58, 71–78.*

Frisch, W., 1979: Tectonic progradation and plate tectonic evolution of the Alps. *Tectonophysics, 60, 121–139.*

Frisch, W. & Gavlick, H. J., 2003: The nappe structure of the central Northern Calcareous Alps and its disintegration during Miocene tectonic extrusion: A contribution to understanding the orogenic evolution of the Eastern Alps. *Int. J. Earth. Sci., 92, 712–727.*

Gawlick, H. J. & Frisch, W., 2003: The Middle to Late Jurassic carbonate clastic radiolaritic flysch sediments in the Northern Calcareous Alps: Sedimenology, basin evolution, and tectonics – an overview. *Neu. Jb. Geol. Paläont., Abh., 230, 2/3, 163–213.*

Gawlick, H. J. & Königshof, P., 1993: Diagenese, niedrig- und mittelgradige Metamorphose in den südlichen Salzburger Kalkalpen – Paläotemperaturabschätzung auf der Grundlage von Conodont Color-Alteration-Index- (CAI-) Daten. *Jb. Geol. Bundesanst., 136, 39–48.*

Gawlick, H. J. & Höpfer, N., 1999: Stratigraphie, Fazies und Hochdruck-Mitteltemperatur-Metamorphose der Hallstätter Kalke der Pailwand (Nordliche Kalkalpen, Österreich). *Z. Dtsch. geol. Gesell., 150, 4, 641–667.*

Gawlick, H. J., Frisch, W., Vecsei, A., Steiger, T. & Böhm, F., 1999: The change from rifting to thrusting in the Northern Calcareous Alps as recorded in Jurassic sediments. *Geol. Rdsch., 87, 644–657.*

Gawlick, H. J., Frisch, S., Hoxha, L., Dumitrica, P., Krystyn, L., Lein, R., Missoni, S. & Schlagintweit, F., 2008: Mirdita Zone ophiolites and associated sediments in Albania reveal Neotethys Ocean origin. *Int. J. Earth. Sci., 97, 865–881.*

Golonka, J., 2002: Plate-tectonic maps of the Phanerozoic. *Spec. Publ. (Soc. econ. Paleontologists Mineralogists Tulsa), 72, 21–75.*

Groshong, R. H., Jr., 1972: Strain calculated from twinning in calcite. *Geol. Soc. Amer. Bull., 82, 2025–2038.*

Groshong, R. H., Jr., 1988: Low-temperature deformation mechanisms and their interpretation. *Geol. Soc. Amer. Bull., 100, 1329–1360.*

Haas, J., Kovács, S., Krystyn, L. & Lein, R., 1995: Significance of Late Permian-Triassic facies zones in terrane reconstructions in the Alpine-North Pannonian domain. *Tectonophysics, 242, 19–40.*

Ivan, P., 2002: Relics of the Meliata Ocean crust: Geodynamic implications of mineralogical, petrological and geochemical proxies. *Geol. Carpath., 53, 245–256.*

Ivan, P. & Méres, Š., 2009: Blueschist enclave in the Dobšiná quarry: The evidence of the relation of the ultrabasic body to the Hačava Fm. of the Bôrka nappe (Meliatic Unit, Slovakia). *Miner. Slov., 41, 4, 407–418.*

Ivan, P., Méres, Š. & Sýkora, M., 2009: Magnesioriebeckite in red cherts and basalts (Jaklovce Fm. of the Meliatic Unit, Western Carpathians): An indicator of initial stage of the high-pressure subduction metamorphism. *Miner. Slov., 41, 4, 419–432.*

Jamison, W. R. & Spang, J. H., 1976: Use of calcite twin lamellae to infer differential stress. *Geol. Soc. Amer. Bull., 87, 6, 868–872.*

Kralik, M., Klima, K. & Riedmüller, G., 1987: Dating fault gouges. *Nature, 327, 6126, 315–317.*

Kozur, H., 1991: The evolution of the Meliata Ocean and its significance for the early evolution of the Eastern Alps and Western Carpathians. *Palaeogeogr. Palaeoclimatol. Palaeoecol., 87, 109–135.*

Lacombe, O., 2007: Comparison of paleostress magnitudes from calcite twins with contemporary stress magnitudes and frictional sliding criteria in the continental crust: mechanical implications. *J. struct. Geol., 29, 86–99.*

Laurent, P., Kern, H. & Lacombe, O., 2000: Determination of deviatoric stress tensors based on inversion of calcite twin data from experimentally deformed monophase samples. Part II. Axial and triaxial stress experiments. *Tectonophysics, 327, 131–148.*

Maluski, H., Rajlich, P. & Matte, P., 1993: ^{40}Ar–^{39}Ar dating of the Inner Carpathians Variscan basement and Alpine mylonitic overprinting. *Tectonophysics, 223, 313–337.*

Mello, J., Reichwalder, P. & Vozárová, A., 1998: Bôrka nappe: High-pressure relic from the subduction-accretion prism of the Meliata Ocean (Inner Western Carpathians, Slovakia). *Slovak Geol. Mag., 4, 261–273.*

Missoni, S. & Gawlick, H. J., 2011a: Evidence for Jurassic subduction from the Northern Calcareous Alps (Berchtesgaden; Austroalpine, Germany). *Int. J. Earth. Sci., 100, 1605–1631.*

Missoni, S. & Gawlick, H. J., 2011b: Jurassic mountain building and Mesozoic-Cenozoic geodynamic evolution of the Northern Calcareous Alps as proven in the Berchtesgaden Alps (Germany). *Facies, 57, 137–186.*

Mock, R., Sýkora, M., Aubrecht, R., Ožvoldová, L., Kronome, B., Reichwalder, P. & Jablonský, J., 1998: Petrology and petrography of the Meliaticum near the Meliata and Jaklovce villages, Slovakia. *Slovak Geol. Mag., 4, 223–260.*

Németh, Z., 1996: First discovery of the Bôrka nappe in the eastern part of the Spiš-Gemer Ore Mts., Western Carpathians. *Miner. Slov., 28, 3, 175–184.*

Németh, Z., 2005: Paleopiezometry: Tool for determination of differential stresses for principal ductile shear zones of Gemericum, Western Carpathians. *Slovak Geol. Mag., 11, 2–3, 185–193.*

Németh, Z., Gazdačko, Ľ., Návesňák, D. & Kobulský, J., 2007: Polyphase tectonic evolution of Gemericum (the Inner Western Carpathians) outlined by review of structural and deformational data. In: Grecula, P., Hovorka, D. & Putiš, M. (eds.): Geological evolution of Western Carpathians. Monogr. *Miner. Slov., 215–224.*

Németh, Z., Radvanec, M., Kobulský, J., Gazdačko, Ľ., Putiš, M. & Zákršmidová, B., 2012: Allochthonous position of the Meliaticum in the North-Gemeric zone (Inner Western Carpathians) as demonstrated by paleopiezometric data. *Miner. Slov., 44, 1, 57–64.*

Németh, Z., Putiš, M. & Hraško, Ľ., 2016: The relation of metallogeny to geodynamic processes – the natural prerequisite for the origin of mineral deposits of public importance (MDoPI): The case study in the Western Carpathians, Slovakia. *Miner. Slov., 48, 119–134.*

Nicolas, J. & Poirier, J. P., 1976: Crystalline plasticity and solid state flow in metamorphic rocks. *London, Wiley.*

Passchier, C. W. & Trouw, R. A. J., 1996: Microtectonics. *Springer, 1–289.*

Plašienka, D., 2018: Continuity and episodicity in the Early Alpine tectonic evolution of the Western Carpathians: How large-scale processes are expressed by the orogenic architecture and rock record data. *Tectonics, 37.*

Plašienka, D., Méres, S., Ivan, P., Sýkora, M., Soták, J., Lačný, A., Aubrecht, R., Bellova, A. & Potočný, T., 2019: Meliatic blueschists and their detritus in Cretaceous sediments: New data constraining tectonic evolution of the West Carpathians. *Swiss J. Geosci., 112, 55–82.*

Putiš, M., Radvanec, M., Sergeev, S., Koller, F., Michálek, M., Snárska, B., Koppa, M., Šarinová, K. & Németh, Z., 2011: Metamorphosed succession of cherty shales with basalt and diastrophic breccia in olistolith of the Meliatic Jurassic accretion wedge near Jaklovce (Slovakia), dated on zircon (U-Pb SIMS SHRIMP). *Miner. Slov., 43, 1–18.*

Putiš, M., Koppa, M., Snárska, B., Koller, F. & Uher, P., 2012: The blueschist-associated perovskite-andradite--bearing serpentinized harzburgite from Dobšiná (the Meliata Unit), Slovakia. *J. Geosci., 57, 221–240.*

Putiš, M., Danišík, M., Ružička, P. & Schmiedt, I., 2014: Constraining exhumation pathway in an accretionary wedge by (U-Th)/He thermochronology – Case study on Meliatic nappes in the Western Carpathians. *J. Geodyn., 81, 80–90.*

Putiš, M., Soták, J., Li, Q.-L., Ondrejka, M., Li, X.-H., Hu, Z., Ling, X., Nemec, O., Németh, Z. & Ružička, P., 2019: Origin and age determination of the Neotethys Meliata Basin ophiolite fragments in the Late Jurassic-Early Cretaceous accretionary wedge mélange (Inner Western Carpathians, Slovakia). *Minerals, 9, 652, 1–38.*

Rannalli, G., 1984: Grain size distribution and flow stress in tectonics. *J. struct. Geol., 6, 443–447.*

Rowe, K. J. & Rutter, E. H., 1990: Paleostress estimation using calcite twinning: Experimental calibration and application to nature. *J. struct. Geol., 6, 443–447.*

Rybacki, E., Evans, B., Janssen, C., Wirth, R. & Dresen, G., 2013: Influence of stress, temperature, and strain on calcite twins constrained by deformation experiments. *Tectonophysics, 601, 20–36.*

Schmid, S. M., Bernoulli, D., Fügenschuh, B., Matenco, L., Schefer, S., Schuster, R., Tischler, M. & Ustaszewski, K., 2008: The Alpine-Carpathian-Dinaridic orogenic system: correlation and evolution of tectonic units. *J. Geosci., 101, 139–183.*

Stöckhert, B., Brix, M. R, Leinschrodt, R., Hurford, A. & Wirth, R., 1999: Thermochronometry and microstructures of quartz – a comparison with experimental flow laws and predictions on the temperature of the brittle-plastic transition. *J. struct. Geol., 21, 3, 351–369.*

Tollmann, A., 1976: Analyse des klassischen nordalpinen Mesozoikums. *Wien, Deuticke, 1–580.*

Tollmann, A., 1977: Geologie von Österreich. Band 1. *Wien, Deuticke, 1–766.*

Turner, F. J., 1964: Metamorphic Petrology: Mineralogy, field and tectonic aspects. *New York, McGraw Hill Book, 339–401.*

Vlahovič, I., Tišljar, J., Velič, I. & Matičec, D., 2005: Evolution of the Adriatic carbonate platform: Paleogeography, main events and depositional dynamics. *Palaeogeogr. Palaeoclimatol. Palaeoecol., 220, 333–360.*

Zulauf, G., 2001: Structural style, deformation mechanisms and paleodifferential stress along an exposed crustal section; constraints on the rheology of quartzfeldspatic rocks at supra- and infrastructural levels (Bohemian massif). *Tectonophysics, 332, 211–237.*

Zákršmidová, B., Jacko, S. & Németh, Z., 2016: Paleopiezometry – the new investigation method applied on the Penninic oceanic suture zone in comparison to the Meliata-Hallsttat suture zone. *Acta Montan. Slov., 21, 43–52.*

Diferenciálne napätia z deformovaných kalcitových žíl vo vysokotlakovo-nízkoteplotne deformovaných triasových hallstattských vápencoch (Severné Vápencové Alpy, Rakúsko)

Aplikovaním metodiky paleopiezometrie sme vypočítali diferenciálne napätia ($\sigma_D = \sigma_1 - \sigma_3$), ktoré zaznamenali zrná v penetratívnych kalcitových žilách prestupujúcich hostiteľskou horninou – vysokotlakovo-nízkoteplotne metamorfovaným hallstattským vápencom (obr. 1 – 3) na lokalite Pailwand v centrálnej časti Severných Vápencových Álp (Rakúsko).

Hallstattský vápenec je interpretovaný ako laterálny ekvivalent karbonatickej sekvencie príkrovu Bôrky meliatika Západných Karpát a bol deformovaný aj počas jursko-spodnokriedového subdukčno-exhumačného procesu. Náš výskum mal za cieľ rozšíriť poznatky o charaktere a parametroch jeho duktilnej deformácie, podobne, ako sme to skôr zistili v príkrove Bôrky. Paleopiezometrické údaje z kalcitických mramorov príkrovu Bôrky zdokumentovali pôsobiace diferenciálne napätia, a to v prípade skôr exhumovaných frontálnych častí príkrovu Bôrky (348 až 430 MPa), rovnako ako z jeho neskôr exhumovaných tylových častí (188 až 278 MPa), ktoré už zaznamenali aj začiatok statickej rekryštalizácie (cf. Németh, 2005; Németh et al., 2012).

V prípade hallstattských vápencov sme zistili, že ich skoršia extrémna duktilná deformácia (obr. 4) spájaná so subdukčným procesom spôsobujúca vznik mylonitových až ultramylonitových deformačných pásov s extrémnou redukciou veľkosti kalcitových porfyroklastov (rozmery max. niekoľko desiatok μm) tvoriacich asymetrické štruktúry, rovnako ako absencia deformačných lamiel v kalcitových zrnách, neumožňuje zrealizovať paleopiezometrické merania a vyčísliť deformačný gradient ich deformácie pri subdukčnom procese.

Dôležité bolo ale zistenie, že hallstattské vápence s už dotvorenou duktilnou stavbou sú prestúpené mladšími kalcitovými žilami, na ktoré po ich vzniku tiež pôsobilo napäťové pole a zaznamenali sukcesívne mladšiu duktilnú deformáciu s diferenciálnymi napätiami 184 až 234 MPa (tab. 1). Túto mladšiu deformačnú epizódu je možné interpretovať ako dôsledok exhumačného procesu, prípadne príkrovového presunu alebo ponásunového odstrešovania. Deformácia kalcitových zŕn v týchto žilách (obr. 5) sa vyznačuje tvorbou vysokého počtu deformačných lamiel v zrnách (21 – 47 lamiel na 1 mm kolmej vzdialenosti oproti lamelám) pri zistenej veľkosti zŕn 323 – 571 μm. Niektoré časti žíl už indikovali aj začiatok statickej rekryštalizácie (polygonizáciu zŕn)

Zrealizovaný výskum a nové paleopiezometrické výsledky z lokality Pailwand diferenciálnymi napätiami zdokumentovali len najmladšiu duktilnodeformačnú udalosť, ale mikroštruktúrne bol zaznamenaný aj mylonitizačný proces hlavnej subdukčnej duktilnej deformácie. Napriek tomu prinášajú ďalší dôkaz o vhodnosti paralelizácie hallstattských vápencov s karbonatickou sukcesiou príkrovu Bôrky a indikujú podobnosť priebehu subdukčno-exhumačného procesu v tejto časti neotetýdnej zóny (obr. 6).

Doručené / Received: 28. 10. 2019
Prijaté na publikovanie / Accepted: 11. 8. 2020